Electronic Supplementary Material (ESI) for Physical Chemistry Chemical Physics.

Supporting information

A density functional theory study of ethylene hydrogenation on MgO and γ-Al_2O_3 supported carbon-containing Ir_4 cluster

Kezhen Qi [1,2], Jin-Mo Zhao [2] and Gui-Chang Wang [2,3*]

([1] College of chemistry and Life Science, Shenyang Normal University, Shenyang, 110034, P. R. China; [2] Department of Chemistry, Tianjin Key Lab of Metal and Molecule-based Material Chemistry and Synergetic Innovation Center of Chemical Science and Engineering (Tianjin), Nankai University, Tianjin 300071, P. R. China; [3] State Key Laboratory of Coal Conversion, Institute of Coal Chemistry, Chinese Academy of Sciences, Taiyuan, 030001, P. R. China)

(1) *Corresponding authors: Gui-Chang Wang. E-mail: wangguichang@nankai.edu.cn

Ethylene hydrogenation on FC defective MgO and the partially hydroxylated γ-Al_2O_3

The catalytic activity of ethylene hydrogenation on FC defective MgO and the partially hydroxylated γ-Al_2O_3 catalysts has been investigated, and the optimized transition state structures as well as some key configurations are given in Figure S9.

a) FC-defected MgO The FC-defected MgO(100) was built by remove the top layer surface oxygen atom attached to the Ir atom. On the defected MgO(100), the adsorption energy of Ir_4 cluster is found to be -4.62 eV, and it is 1.30 eV more stable than that of perfect MgO(100), which means that the oxygen vacancy can enhance the adsorption of Ir_4 cluster. Due to the stronger binding of the Ir_4 cluster on the MgO support in the presence of oxygen vacancy, adsorption of adsorbated species on Ir_4 cluster would be weaker, hence the lower energy barrier for the hydrogenation reaction can be expected. Indeed, the calculation results show that the energy barrier of the first hydrogenation step is 0.12 eV lower compared to that of ideal MgO(100), and this reaction step is endothermic by 0.71 eV. For the second hydrogenation step, however, the activation energy is very close to the situation of perfect MgO(100) (1.02 eV on oxygen vacuum MgO(100) and 1.04 eV on perfect MgO(100)). These calculation results indicated that the oxygen vacuum has the ability to enhance the first hydrogenation step and changed a little for the second hydrogenation step. In fact, similar result has been gained in our previous study on acetylene hydrogenation on anatase TiO_2(101)-supported Pd_4 cluster, in which it is found that the Pd_4 cluster on oxygen-defected surface of anatase TiO_2(101) shows higher activity for acetylene hydrogenation than that of perfect anatase TiO_2(101)-supported Pd_4 cluster.[1,2]

b) Hydroxylated γ-Al_2O_3 Digne et al.[3] found that the perfect γ-Al_2O_3 (110) surface is less stable than that of (100) face due to it higher surface energy, and it would become more stable when the (110) surface is hydroxylated. So it is necessary to study the process of hydroxyl formation on

γ-Al_2O_3(110), which proceed via water dissociation ($H_2O \rightarrow H+OH$), at first. The calculation results show that the water dissociation process is exothermic by 0.25 eV, and the corresponding reaction barrier is 0.30 eV. Since the reaction barrier is relatively low, one can expect that the OH species can be produced on γ-Al_2O_3(110) with high efficiency. At the TS, the OH-H bond length is 1.39Å, and the associated imaginary frequency is 965 icm^{-1}. The dissociated OH intermediate binds to surface Al atom and the H atom binds to the surface O atom, giving a total of two OH groups on γ-Al_2O_3(110). After confirming the presence of OH species, the adsorption of Ir_4 cluster on hydroxylated γ-Al_2O_3 has studied. It is found that the calculated Ir_4 cluster binding energy is smaller than that of perfect γ-Al_2O_3(110) (-4.82 eV vs. -5.02 eV), which means that the presence of hydroxyl can inhibit the adsorption of Ir_4 cluster on γ-Al_2O_3(110). Based on the hydroxylated γ-Al_2O_3(110) model, the adsorption properties of hydrogen atom and ethylene, and the subsequent hydrogenation processes of ethylene on γ-Al_2O_3(110) at low hydrogen coverage (*i.e.*, one H_2 molecule on per Ir_4 cluster) were explored. The first hydrogenation step is calculated to be of the energy barrier of 0.88 eV, and the second hydrogenation step has the activation barrier of 0.60 eV. Clearly, both of these two steps has higher energy barrier than the ideal γ-Al_2O_3(110), hence a lower activity for ethylene hydrogenation into ethane.

In a short summary, if the hydroxyl presence on γ-Al_2O_3(110) and the oxygen defect on MgO(100) are taken into account, one can find that the catalytic activity difference for ethylene hydrogenation into ethane would only be changed by a non-significant amount, namely from 1.04 eV to 1.02 eV for defective MgO(100) and from 0.78 eV to 0.88 eV for hydroxylated γ-Al_2O_3(110). So the relative order of the activity are consistent with our above analysis without taken into account the surface defects and hydroxylation into consideration.

References

(1) Yang, J.; Cao, L.-X.; Wang, G.-C. *J Mol Model.* **2012**, *18,* 3329-39.

(2) Yang, J.; Lv, C.-Q.; Guo, Y.; Wang, G.-C. *J. Chem. Phys.* **2012**, *136*, 104107-14.

(3) Digne, M.; Sautet, P.; Raybaud, P.; Euzen, P.; Toulhoat, H. *J. Catal.* **2004**, *54*, 226-229.

(2) Micro-kinetic simulation

In order to connect the calculated microscopic behavior of the cluster and the adsorbates to the observed macroscopic catalytic behavior, and to verify the previous assessment of catalytic activity by the energy span quantity, simulation is conducted. Since the high barrier and thus the low frequency for the transformations of chemical interest prohibits a direct molecular dynamics simulation on the time evolution of the system, the kinetic Monte Carlo simulation, which has been used for the study of surface catalytic behavior for a long time[1] and is shown to be able to give results with great accuracy,[2,3] is usually resorted to tackle this kind of “rare event” problem . For the simulation of extended surfaces, the explicit consideration of the microscopic nano-scale structure of the surface in the kMC simulation makes it give different and far more accurate results than the traditional mean-field simulation.[5] But in the system composed of tetrairidium cluster scattered on the support in this study, each cluster can be considered to behave independently because of the small amount of the cluster on support and thus the long average distance between them in the experiments.[6] As a result, rather than a normal kinetic Monte Carlo study where the exact state of a set of active sites is explicitly considered for the description of the state of the system, the state of the catalytic system is specified by an *n*-dimensional vector in this study, where *n* is the number of possible states for each cluster. The components of the vector gives the fractional occupation number of each possible state of the cluster in an infinite ensemble of clusters, and the time evolution of the system is obtained by simulating the trajectory of this vector. It can be readily proved mathematically that for independent active sites, this description is the limit that a normal kinetic Monte Carlo simulation converges to when the number of simulated active sites approaches infinity. Due to the number of ethylene and hydrogen molecules on the cluster that is considered in the DFT study, in the simulation, the states of the clusters are limited to the set in which merely at most one ethylene molecule and two hydrogen molecules have been adsorbed onto the cluster. Because of the high mobility of the hydrogen atom on the cluster, each state for the cluster is specified by only the number and position of the ethylene-derived group and the number of hydrogen atoms directly adsorbed on the cluster. The system is then considered to be dominantly in the lowest-energy configuration that is consistent with the specification of its state in this way. Then for the MgO supported cluster, eight states of the clusters are considered. If a tuple (*a*, *b*, *c*) denotes the state of the cluster with *a* adsorbed ethylene molecule on one of the equivalent *a*-Ir atom, *b* adsorbed hydrogen atomand *c* adsorbed ethyl group, then the eight states can be enumerated as (0,0,0), (1,0,0), (0,2,0), (1,2,0), (0,1,1), (0,4,0), (1,4,0), (0,3,1). For the γ-Al_2O_3 supported case, the number of all possible states increase by an amount of five because of the loss of symmetry and equivalency of the two *a*-Ir atoms and thus the presence of two possible sites for the ethylene-derived groups. M.C. to make the simulation of the adsorption and desorption evens converges to the correct thermodynamic equilibrium when the simulation time tends to infinity, namely

$$r^{des} = r^{ads} \frac{q_{subst}^{vib}}{q_{ads}^{vib}} q_i^{trans} q_i^{rot} q_i^{vib} \exp(-\frac{E_{des}}{k_B T}) , \qquad (2)$$

where the q_i^{trans}, q_i^{rot} and q_i^{vib} denote the translational, rotational and vibrational partition function of the adsorbate molecule in gas phase and q_{subst}^{vib} and q_{ads}^{vib} are the vibrational partition function of the composite system after the adsorption and the vibrational partition function of the substrate. r^{ads} denotes the rate for the corresponding adsorption process and E_{des} is the desorption heat. This way of treating rates of adsorption and desorption evens is able to make the simulation consistent with thermodynamic equilibrium and have been shown to be able to reproduce experimental results very well. For reactions, the rates are calculated by the Eyring equation

$$r^{reac} = \frac{q_{TS}^{vib}}{q_{TS}^{vib}} (\frac{k_B T}{h}) \exp(-\frac{E_a}{k_B T}) , \qquad (3)$$

where E_a is the activation energy from DFT computations with zero-point energy correction being applied to the barrier of the hydrogenation reactions at higher hydrogen coverage due to their dominance and thus importance in determining the activity of the catalysts, and q_{TS}^{vib} and q_{TS}^{vib} are the vibrational partition function of the transition and initial state. If the reaction requires some pre-activation prior to the real reaction, a factor *f*, which gives the fraction of the activated precursor in the stationary configurations of the state according to Maxwell-Boltzmann distribution, is multiplied to the result of the Eyring function. The time evolution of the system is reduced to the propagation of the state vector in an autonomous way by equation dr/dt = Ar, where r gives the state of the system and A is a matrix whose non-diagonal elements Ai, j is the transition rate from state j to state i of the cluster and whose diagonal elements **A**k, k is the negative of the sum of all the escape rates from state k of the cluster.

References

(1) Hansen, E. W.; Neurock, M. *Chem. Eng. Sci.* **1999**, *54*, 3411-3421.

(2) Reuter, K.; Frenkel, D.; Scheffler, M. *Phys. Rev. Lett.* **2004**, *93*, 116105-4.

(3) Reuter, K.; Scheffler, M. *Phys. Rev. B* **2006**, *73*, 045433-17.

(4) Henkelman, G.; Jonsson, H. *J. Chem. Phys.* **2001**, *115*, 9657-9666.

(5) Temel, B.; Meskine, H.; Reuter, K.; Scheffler, M.; Metiu, H. *J. Chem. Phys.* **2007**, *126*, 204711-12.

(6) Argo, A. M.; Odzak, J. F.; Lai, F. S.; Gates, B. C. *Nature* **2002**, *415*, 623-626.

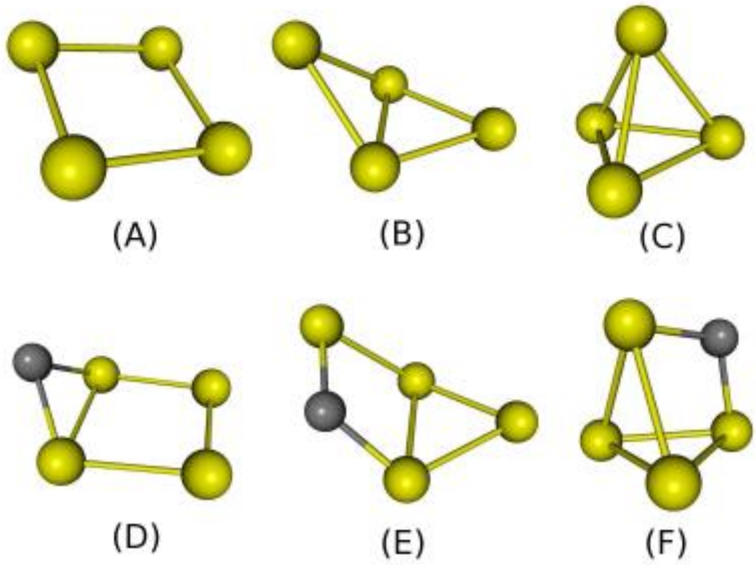

Figure S1 Various configurations for the tetrairidium cluster in the gas-phase: (A), (B) and (C) shows the planar, butterfly and tetrahedral configuration, respectively, without the pre-adsorbed carbon atom. (D), (E) and (F) give the corresponding structures with the carbon atom.

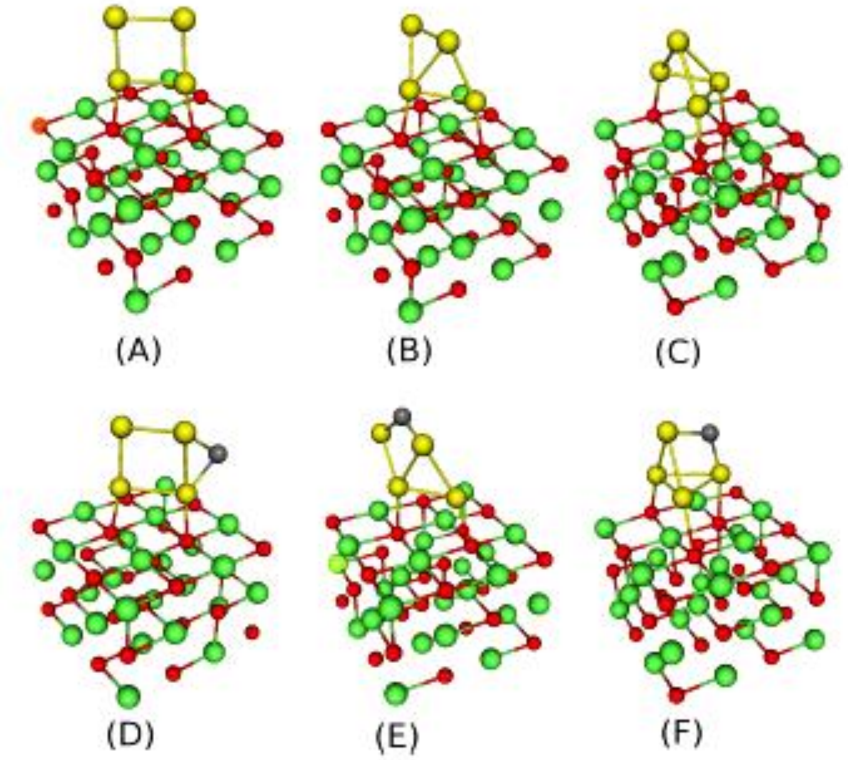

Figure S2 Various configurations for the tetrairidium cluster on the MgO(100) surface: (A), (B) and (C) shows the planar, butterfly and tetrahedral configuration, respectively, without the pre-adsorbed carbon atom. (D), (E) and (F) give the corresponding structures with the carbon atom.

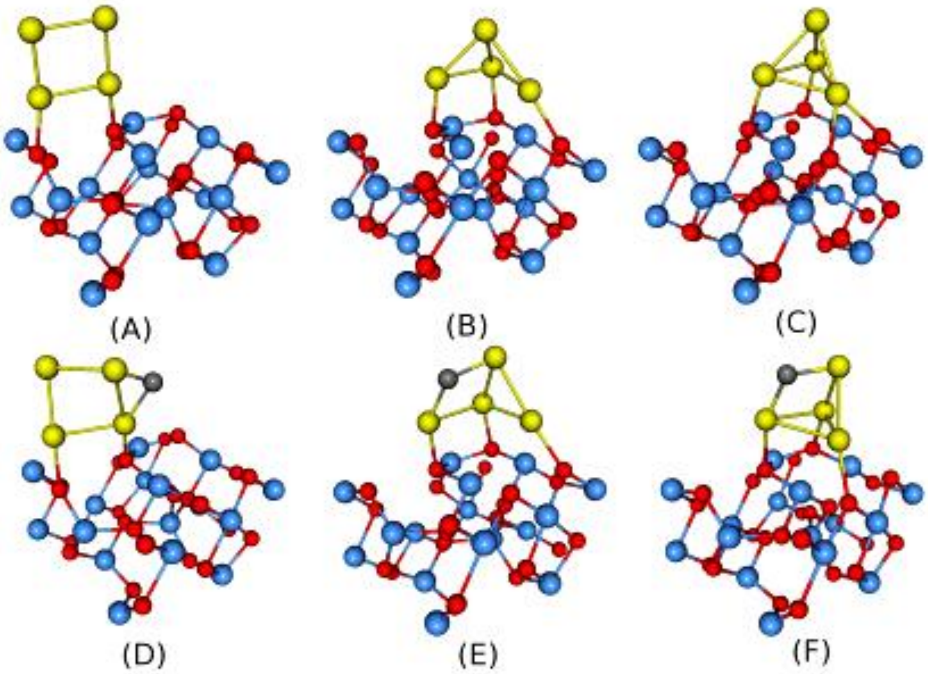

Figure S3 Various configurations for the tetrairidium cluster on the γ-Al_2O_3(110) surface: (A), (B) and (C) shows the planar, butterfly and tetrahedral configuration, respectively, without the pre-adsorbed carbon atom. (D), (E) and (F) give the corresponding structures with the carbon atom.

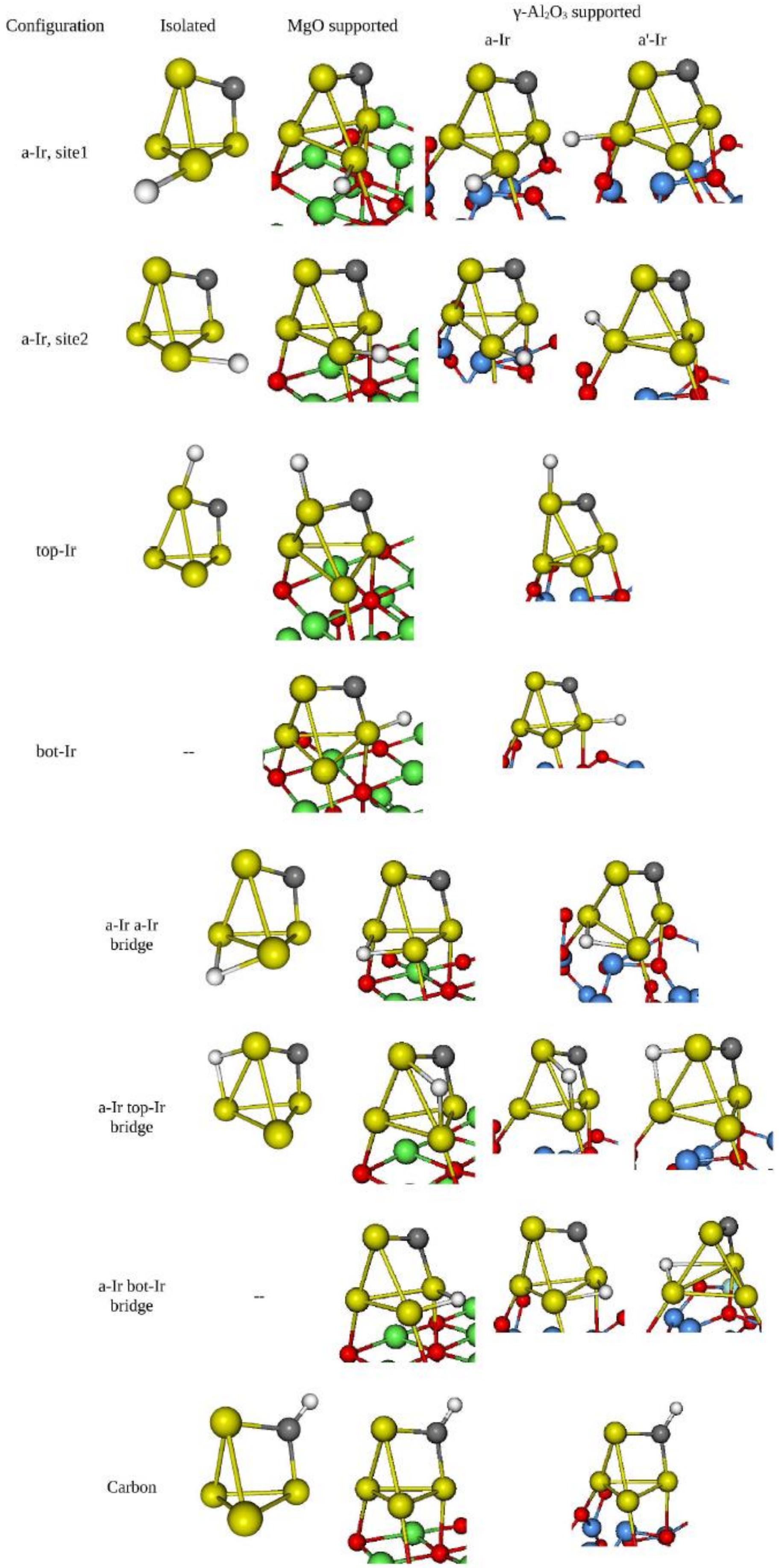

Figure S4 The structures of the various adsorption mode of the hydrogen

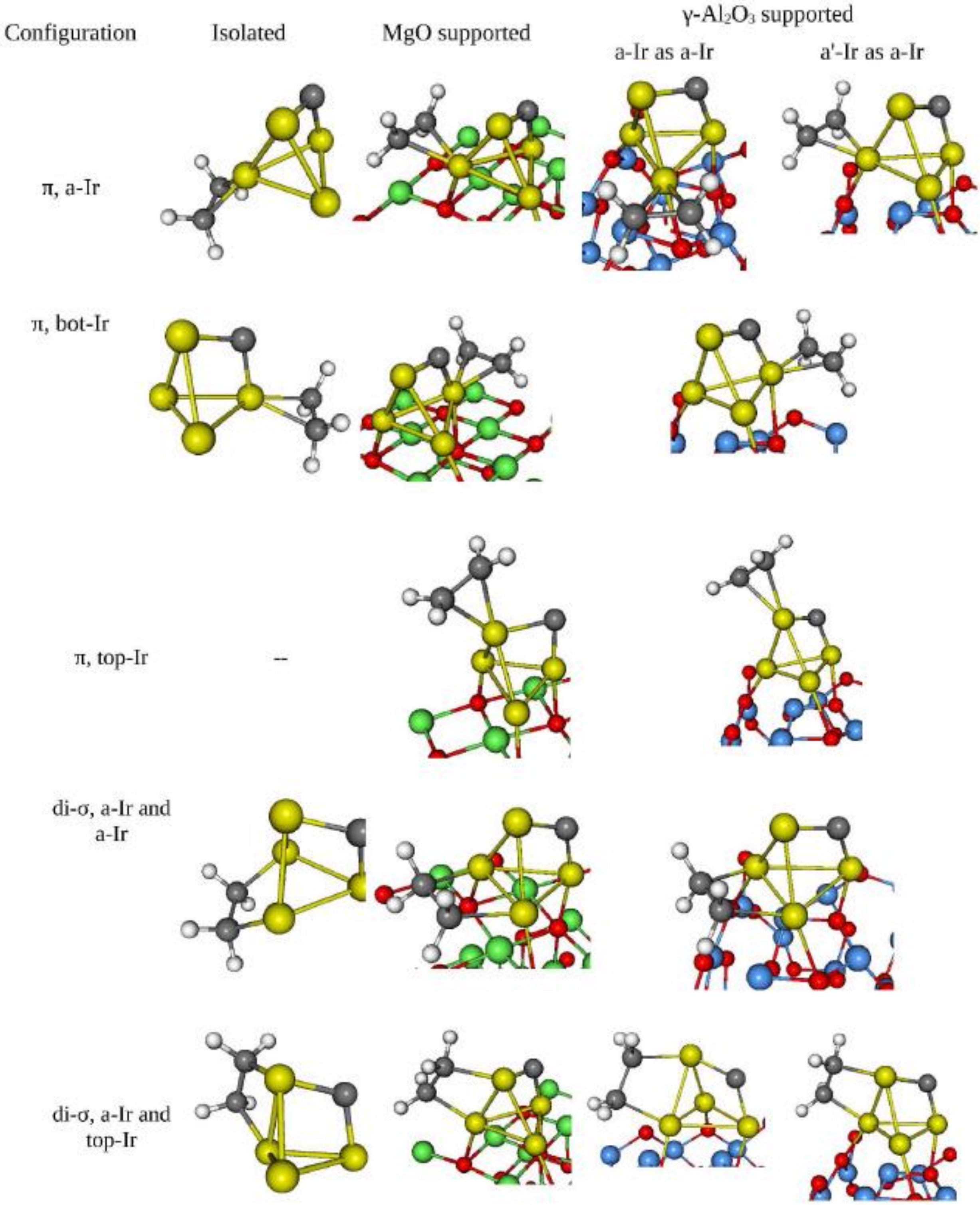

Figure S5 The structures of the various adsorption mode of the ethylene molecule

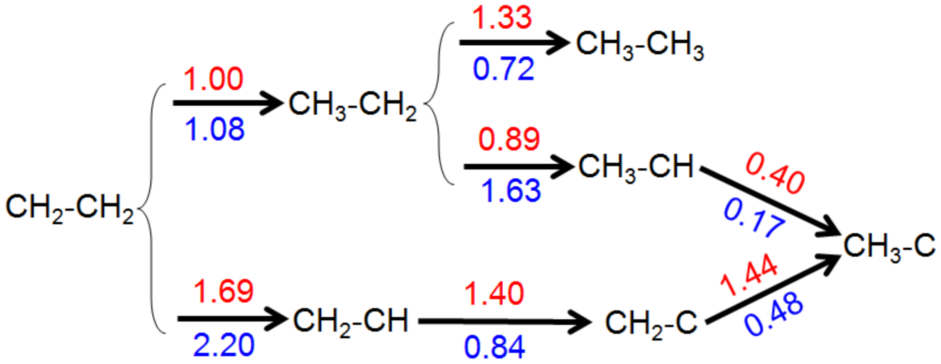

Figure S6 Reaction pathway: blue for the activation energy on MgO(100) support, red for the activation energy on Al_2O_3(110) support at low hydrogen coverage

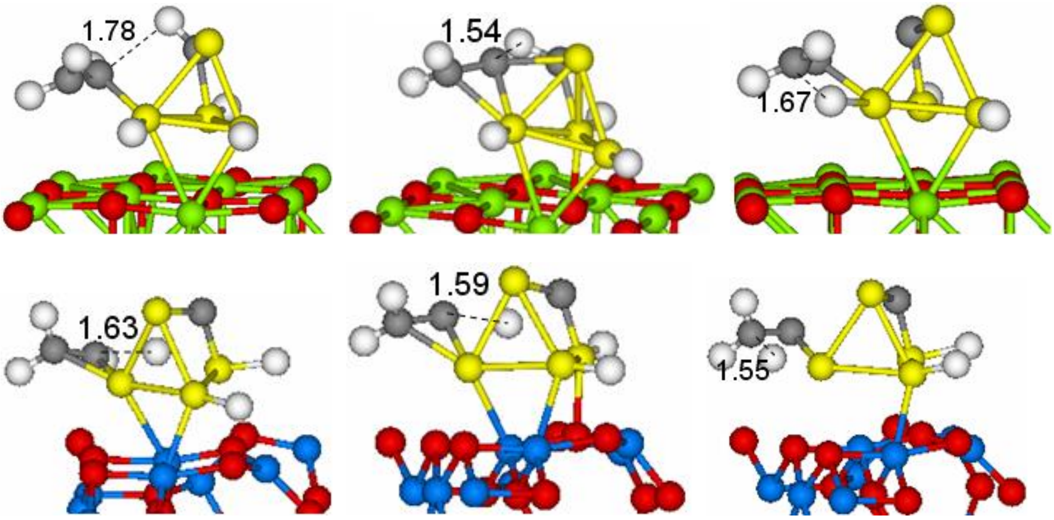

$CH_2CH_2 \rightarrow CH_2CH+H$ $CH_2CH \rightarrow CH_2C+H$ $CH_2C+H \rightarrow CH_3C$

Figure S7 Transition state structures of C-H breaking on MgO(100) and γ-Al_2O_3(110) with low hydrogen coverage

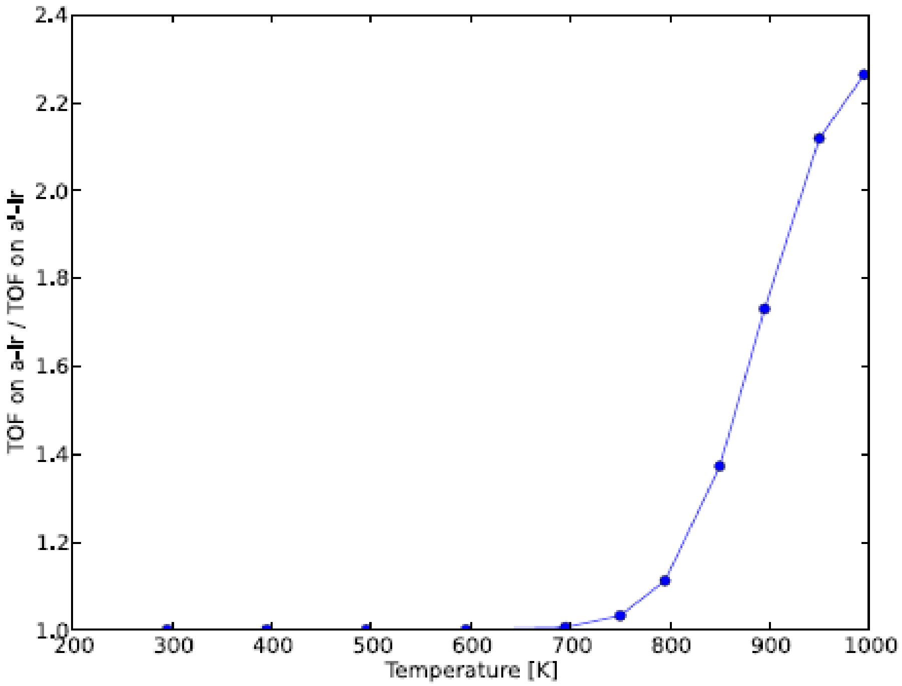

Figure S8 The ratio of the contribution to the TOF by ethylene molecules on *a*-Ir to that by ethylene molecules on *a′*-Ir.

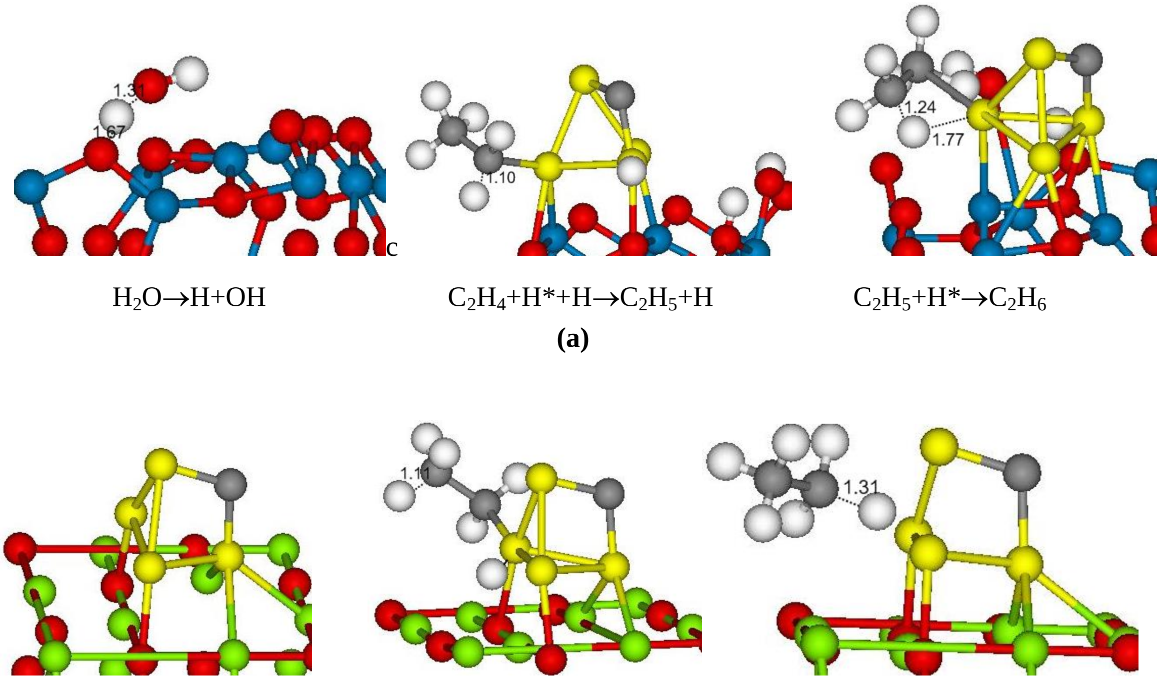

$H_2O \rightarrow H+OH$ $C_2H_4+H^*+H \rightarrow C_2H_5+H$ $C_2H_5+H^* \rightarrow C_2H_6$

(a)

Ir_4 $C_2H_4+H^*+H \rightarrow C_2H_5+H$ $C_2H_5+H^* \rightarrow C_2H_6$

(b)

Figure S9 Transition state structures of ethylene hydrogenation on hydroxylated (a) γ-Al_2O_3(110) and (b) oxygen-defect MgO(100).